Proceedings of the 2019 5th International Conference on Advances in Electrical Engineering (ICAEE)
26-28 September, Dhaka, Bangladesh

Bandwidth-Enhanced Metamaterial Integrated Antenna for Wireless Applications

Nipa Dhar[1], Muhammad Asad Rahman[1], Md. Azad Hossain[1], and Ahmed Toaha Mobashsher[2]
[1]*Faculty of Electrical and Computer Engineering, Chittagong University of Engineering and Technology, Bangladesh*
[2]*School of Information Technology and Electrical Engineering, The University of Queensland, Australia*
nipa@cuet.ac.bd, asad31@cuet.ac.bd, azad@cuet.ac.bd, a.mobashsher@uq.edu.au

***Abstract*—This paper represents a metamaterial (MTM) integrated bandwidth-enhanced antenna for modern wireless communication systems. The MTM ultra wide-band (UWB) antenna comprises of two unit cells on the top of the substrate, a circular disc monopole, and a partial ground plane. The unit cell consists of a split ring resonator. Without unit cells, the monopole antenna can operate in a wide band of impedance bandwidth of 7.5 GHz, corresponding to a percentage bandwidth of 120% (2.5-10 GHz). After the integration of MTMs, the proposed antenna can operate from 1.5-10 GHz range with a percentage bandwidth of 147.8%. So, MTMs integration can provide additional operation at 1.5-2.5 GHz, thus the bandwidth is broadened. As the dimensions of the unit cells are much smaller than the resonant frequency, miniaturization of the antenna size can be achieved. Different simulated antenna performance parameters such as reflection coefficients, radiation patterns, and gain are analyzed. The simulated gains of the proposed design at 1.5, 2.4, 5.8 and 10 GHz are 1.17 dBi, 2.18 dBi, 3.6 dBi, and 4.05 dBi, respectively. The proposed antenna could be a potential contender for different remote correspondence frameworks, for example, GPS, Wi-Fi, WLAN, and RADAR.**

Keywords—metamaterial antenna, negative index material, split ring resonator, unit cell, UWB

I. INTRODUCTION

Wireless communication system greatly affects the improvement of present day innovation. So the use of fewer or single antenna for various applications is more efficient. As a result, antennas with very large bandwidth are in great demand. An ultra wide-band (UWB) antenna technology having frequency band in the range of 3.1 to 10 GHz, can be a favorable solution for future wireless communication system due to its high data transfer rate, low power requirement, and invulnerability to multipath interference. A UWB antenna can be appropriate for numerous applications, for example, remote applications, indoor applications, and medical imaging [1]. The advantages of microstrip antenna, for example, low volume, light weight, simple creation, conformal design and similarity with incorporated circuit make them alluring for UWB applications [2]. However, the natural disadvantage of the microstrip antenna is narrow bandwidth (BW). Hence, the impedance bandwidth needs to be improved for UWB applications.

Numerous techniques have been described in [3-4] to increase the bandwidth. Mainly slot-loading techniques have been proposed here. However, slot-loaded techniques such as V-slot patch antenna [3], S-slot patch antenna [4] requires high substrate thickness and large in size. Modern wireless communication devices are getting small. So the miniaturization of the antenna is necessary.

The size reduction of the antenna needed high dielectric material. But these conventional approaches result in the drawbacks [2]. In high permittivity medium, the characteristic impedance is low which causes difficulties in impedance matching and highly concentrated e.m.f. due to large permeability. To overcome these problems, the use of metamaterials (MTMs) is increased. Metamaterial was first discovered by Victor Veselago [5] in 1967. Metamaterials are artificial arrangement of unit cells with properties different from the naturally available materials. The measure of the unit cell is a lot littler than the light wavelength. The electromagnetic property of a medium can be defined by the permeability and permittivity of the medium. The regular materials have positive electrical permittivity, attractive penetrability, and refraction index while the metamaterials have been portrayed as negative index materials (NIM) or double negative (DNG) media or left-handed materials (LHM) having every one of these parameters negative. In this kinds of material, the group velocity is antiparallel to its phase velocity. As a result, backward wave propagation occurred which violates the Snell's law and Cherenkov radiation [6].

Compared to the convention antennas, metamaterial antenna acts much larger as its genuine size because of its artificially designed structure reradiates and stores energy. This feature of metamaterial reduced reflection loss. Mainly, to design zeroth-order-resonant antennas with compact dimensions, epsilon negative transmission line (ENG-TL) offers a way. But normally undergo narrow bandwidth and low radiation efficiency [7]. Recently, several works have been explored in [7-12] to increase the bandwidth. An epsilon negative bandwidth-enhanced zeroth-and first-order resonant antenna has been reported in [7]. This design provides size reduction and higher bandwidth and also efficient for the modern wireless communication system (GSM, UMTS, WLAN, WiMAX). A compact microstrip antenna with enhanced bandwidth has been reported in [8]. By loading magneto-dielectric (MDE) MTM, a relative 3.2% BW can be achieved. But the main drawback is of being high profile. In [9], merging two resonant frequencies of MTMs, BW enhancement has been done. An antenna composed of two resonators and two TL- MTM arms is used to increase the BW but TL-MTM causes the increase in overall size. A metamaterial antenna combines two closely spaced ZOR and first negative order resonant (FNOR) modes by integrating chip-inductor TL, results in widen bandwidth [10]. By using tuning stub and creating defects in the ground plane extended BW achieved in [11-13]. Using a partially reflective metasurface as superstrate, a CP Fabry Perot antenna extended

978-1-7281-4934-9/19/$31.00 ©2019 IEEE

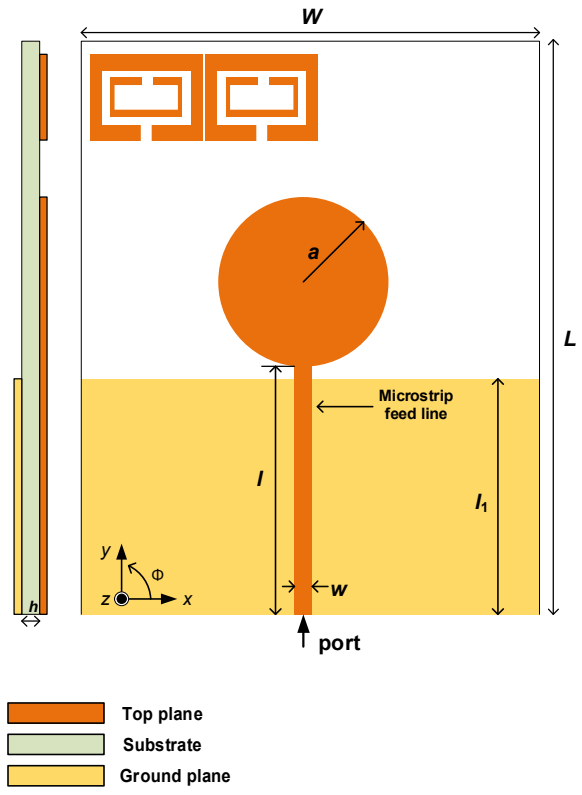

Fig. 1. The configuration of the proposed design.

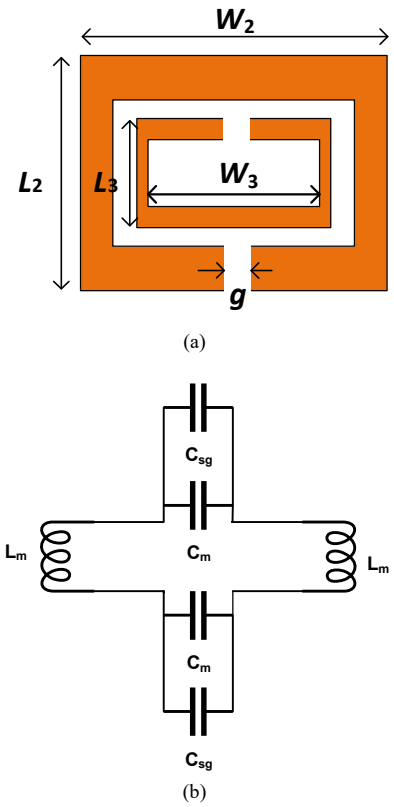

Fig. 2. (a) Metamaterial unit cell. (b) Equivalent circuit.

its impedance bandwidth up to 31.83% (around 15.13% increase in percentage BW) and axial ratio bandwidth up to 10.8% (around 9.2% increase in axial ratio BW) which is depicted in literature [14]. A tri-ring CSRR based antenna is reported in [15], where bandwidth is upgraded from 2.2 to 16%. Here, the split gap of the two inner resonators is rotated in an angle of 0°, 30°, and 60° manner keeping the outer CSRR fixed. Bandwidth up-gradation of a 2 × 2 array antenna is accomplished by integrating two spiral ring resonator reported in [16]. Without spiral resonator, the operating BW of the antenna is 400 MHz but integration of spiral resonator causes BW reached at 700 MHz at 5.8 GHz resonant frequency. A technique illustrated in [17] is used to improve the BW of the microstrip patch antenna. Several irregular shaped pattern is etched on the top patch and the ground plane is replaced by a grid-shaped periodic structure. The improvement in BW reported by the authors in a span of 2.9 to 33.7 GHz. A microstrip patch antenna having a disconnected U-shaped ground and an additional slot in the top patch are used to increase the bandwidth reported in [18]. This dual-band antenna achieved 115 MHz impedance BW at 3.22 GHz and 70 MHz impedance BW at 3.65 GHz, respectively.

This paper investigates the bandwidth enhancement of an ultra wide-band antenna in the lower frequency region. The enhancement of BW can be achieved by manipulating the behavior of ZOR and FOR. As the resonant frequencies of metamaterials are independent of the electrical length of the antenna but determined only by the series and shunt reactance of the antenna, their lies a big opportunity for bandwidth enhancement. In this paper, the circular disc monopole antenna operates in the 2.5-10 GHz frequency range. A planar MTM design (array of 1 × 2) is mounted on the right side of the top of the substrate to upgrade the radiation and to increase the working bandwidth, which frames a capacitance and produces a coupling between the electric fields to make electric resonances. Integration of unit cells operating at lower frequencies than UWB monopole causes the broadband behavior the proposed antenna. Integration of metamaterials causes the zeroth-order resonance creates in the lower frequency band. So, without increasing the size of the antenna, the proposed design can operate in lower bands. Bandwidth enhancement of 27.8% is achieved after metamaterial integration. Along with the UWB applications, the proposed antenna can be used for various wireless applications such as GPS, Wi-Fi, WLAN.

II. Antenna Design

The proposed antenna is a basic UWB antenna loaded with metamaterial unit cells as presented in Fig. 1. Without unit cells, the UWB antenna made up of a circular disc monopole of radius a as a radiating element and a partial ground plane of width W and length l_1. To feed the antenna, a microstrip feed line is used having length l and width w. The radiating element is printed on a dielectric substrate (Rogers RO4003) with relative permittivity of 3.38 and a thickness of 2.1 mm. The overall size is 42×50 mm^2. Two unit cells of metamaterial are placed on the top of the substrate.

The structure perspective on proposed planar-rectangular, left-handed, metamaterial SRR unit cell and its equivalent circuit are appeared in Fig. 2. The ideal objective of the unit cell is to achieve resonance inside the frequency band 1–3 GHz. The unit cell is involved two copper strip ring patches with a thickness of 0.035 mm and having two split gaps (g). A magnetic field is instigated in the SRR which is in charge of making negative permeability. The split gaps (g) in each ring

TABLE I. DIMENSIONS OF THE PROPOSED ANTENNA

Parameter	Dimension (mm)	Parameter	Dimension (mm)
a	10	L_2	8
W	42	L_3	5
L	50	W_2	10
l	20	W_3	8
w	2.6	g	1
l_1	17	h	2.1

instigate an arrangement capacitance which controls the characteristics of resonance. The coupling between the internal and external rings get expanded by the modification of the length and width of the SRR structure and also diminishes the arrangement capacitance. The presentation of the inward square shape and the improvement of the separation between the stripes demand that the unit cell gets the full UWB band. The design parameters are depicted in TABLE I.

The equivalent circuit of SRR is a LC tank circuit, in which the ring acts as an inductor and the gap acts as a capacitor [19]. When the H-field is parallel to the ring axis, it generates a current in the ring. As a result, strong magnetic dipole creates magnetic resonance. And when E-field is parallel to the gap of SRR, voltage variation give rise in the gap and causes electric resonance. By changing the property of the artificial line the magnetic and electric resonance of the unit cell can be created at two closely spaced frequencies. This principle is used in the proposed design to increase the bandwidth. The association between these two metal rings is through a common capacitor. In expansion, each ring looks like a solenoid that can be spoken to by an inductance L_m. The space between the two rings is demonstrated by a capacitor C_m. The split gap capacitor C_{sg} varies inversely with g. The resonant frequency of the SRR is identified with its physical measurements by the accompanying condition given by equation (1)

$$f_{srr} = \frac{1}{2\pi\sqrt{L_m(C_m + C_{sg})}} \tag{1}$$

The MTM unit cell is simulated utilizing computer simulation technology (CST). The unit cell is put between two waveguide ports along the negative and positive x-axis. The ideal electric limit is put opposite to the y-axis, though the perfect magnetic limit is opposite to the z-axis. Fig. 3 demonstrates the behavior of the unit cell. Fig. 3(a) demonstrates the current flow of the proposed LHM unit cell. The flow of current is large over the external stripe. In each stripe, the direction of current flow is opposite because of the changed assembly of the SRRs. The contrary current of the internal and external stripes makes the stopband. By utilizing Nicolson–Ross–Weir approach [6], the viable parameters, for example, the relative permittivity (ε_{eff}), the permeability (μ_{eff}) and refractive index (η) can be recover.

The unit cell is designed for 1.75 GHz where permittivity, permeability, and refractive index are negative. The magnitude of negative permeability (μ_{eff}) is from 1.668 GHz to 1.85 GHz for the unit cell. The negative permittivity (ε_{eff}) is displayed from 1 GHz to 2.64 GHz as appeared in Fig. 3(b). The negative refractive index (η) is appeared 1 GHz to 1.79 GHz, covering a bandwidth of 0.79 GHz.

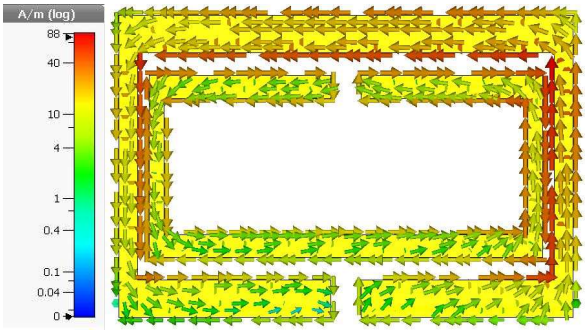

(a)

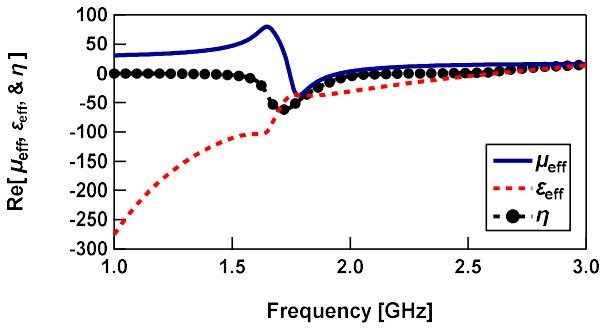

(b)

Fig. 3. (a) Surface current distribution and (b) real part of permittivity, permeability, and refractive index of the unit cell.

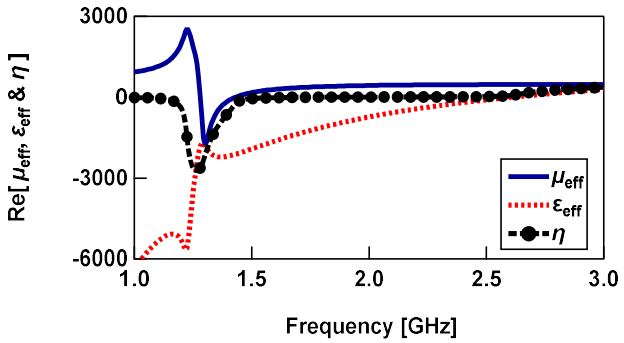

Fig. 4. Real part of permittivity, permeability, and refractive index of 1×2 array of unit cell.

For the 1×2 array of unit cell, the magnitude of negative permeability (μ_{eff}) is from 1.28 GHz to 1.53 GHz. The negative permittivity (ε_{eff}) is displayed from 1 GHz to 2.6 GHz as appeared in Fig. 4. The negative refractive index (η) is appeared 1 GHz to 2.2 GHz having a bandwidth of 1.2 GHz. So, the proposed 1×2 array of unit cell exhibits double negative metamaterial characteristics at 1.5 GHz.

III. PARAMETRIC ANALYSIS

With the purpose of finding the influences on the impedance bandwidth of relating fundamental parameters, a study is done. The variation of the impedance bandwidth with the presence of the metamaterial array of the unit cell and without the unit cells is depicted in Fig. 5. By varying the ratio of W_2 and W_3, keeping all other parameters constant, a parametric analysis is done to find the optimum result. Without the array of unit cells, the operating bandwidth is 7.5

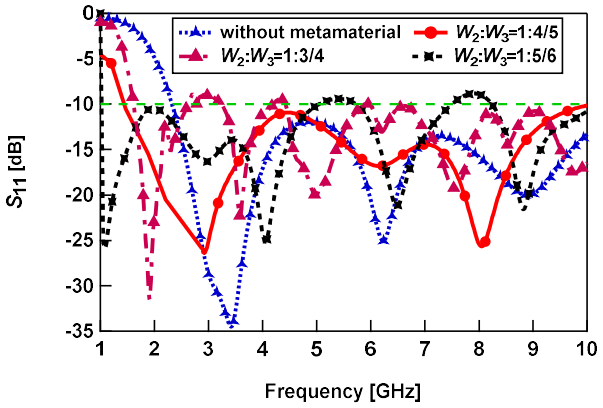

Fig. 5. Variation of impedance bandwidth with the variation of the ratio of W_2: W_3.

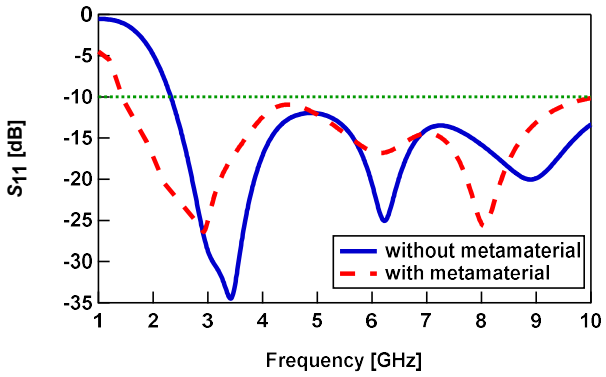

Fig. 6. Reflection co-efficient curve of the proposed antenna.

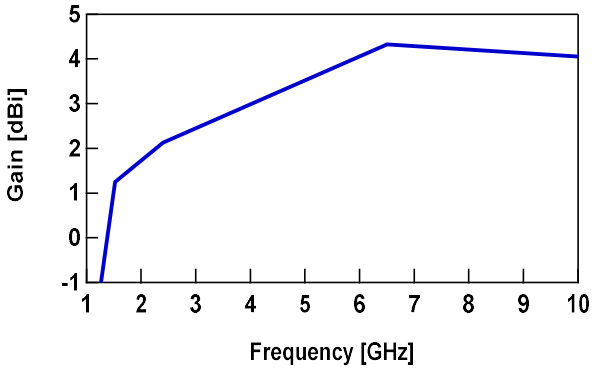

Fig. 7. Gain of the proposed antenna.

GHz equivalent to a percentage bandwidth of 120%. When the ratio of W_2: W_3 is greater than 1: 4/5, impedance bandwidth gets widen in the lower frequency region (1~3 GHz) but reflection coefficient is greater than –10 dB. The same change is observed when the ratio of W_2: W_3 is lower than 1: 4/5. So, the optimum dimensions are W_2 = 10 mm and W_3 = 8 mm. The proposed antenna shows an impedance bandwidth of 8.5 GHz equivalent to a percentage bandwidth of 147.8%.

IV. Simulation Results and Discussion

In Fig. 6, the reflection co-efficient curve of the proposed antenna is shown. Without metamaterial unit cells, the operating bands can cover 2.5 GHz to 10 GHz (–10 dB

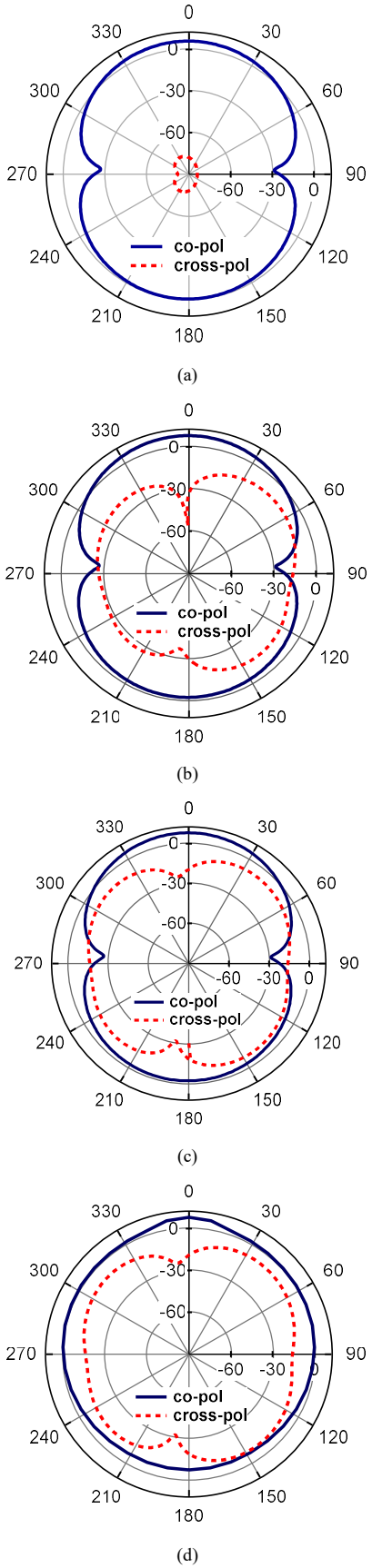

Fig. 8. Radiation pattern of the bandwidth-enhanced antenna in the *x*-*z* plane. (a) 1.5 GHz, (b) 2.4 GHz, (c) 5.8 GHz, and (d) 10 GHz.

TABLE II. COMPARATIVE STUDY OF THE BANDWITH IMPROVEMENT TECHNIQUES

Reference	Year	Technique	Substrate	Operating BW (GHz), %	Gain (dBi)	Antenna Size (λ_o)
[7]	2015	MDE substrate	F4B	3.35-3.72, 10.45	3-5	0.472 × 0.59
[9]	2009	TL-MTM structure	Rogers RT/duriod 588	3.23-3.33, 3.05	0.79	0.437 × 0.437
[11]	2018	Finger-shaped stub	FR4	3-12, 120	2-6	1 × 0.875
[12]	2008	I-shaped dual Slot	RT-Duroid	7.2-12, 50	2.2-3.5	1.09 × 0.928
[13]	2019	Defected ground structure	FR4	3.5-14.5, 122.2	1.5-4.8	0.78 × 0.9
[14]	2019	Partially refractive surface	FR4	5.31-7.33, 31.83	13.33	2.63 × 2.63
[15]	2019	Tri-ring CSRR	-	2.5-2.95, 16	-	-
[16]	2018	Spiral SRR	FR4	5.3-6, 12.38	7.15	-
[18]	2018	Disconnected U-shaped ground	FR4	3.19-3.33, 4.4	-	0.768 × 0.936
Proposed design	2019	Split ring resonators	Rogers RO4003	1.5-10, 147.8	1.17-4.05	0.805 × 0.958

impedance BW = 7.5 GHz) equivalent to a percentage bandwidth of 120%. After the integration of two unit cells, the operating band shifted to the lower frequency band. The new impedance bandwidth of the antenna after integrating 1×2 MTM array is 1.5 GHz to 10 GHz (impedance BW = 8.5 GHz) equivalent to a percentage bandwidth of 147.8%. Finally, the percentage increase in bandwidth is 27.8%.

Fig. 7 represents the simulated gain of the proposed antenna. The gain of the antenna in the lower frequency band (1.5 GHz~2.5 GHz) is about 1.17~2.18 dBi, while in the higher frequency band (3.1~10 GHz) is 2.65~4.05 dBi. In the lower frequency band, the gain is low because the physical size of the antenna is lower than the resonant frequency. The size of the dipole antenna is half of its wavelength and maximum gain is around 2.23 dBi. But the proposed antenna is smaller than its actual size. As a result, gain decrease in the lower frequency band (1.5 GHz~2.5 GHz). The simulated radiation patterns for four different frequencies (1.5, 2.4, 5.8, and 10 GHz) in the *x-z* plane are shown in Fig. 8. From the simulated radiation patterns, it is clear that the isolation between co-polarizations and cross-polarizations are greater than 20 dBi and nearly omnidirectional radiation pattern is obtained for each frequency. By utilizing the 1×2 array of unit cell, the current flowing through feedline does not get diverged and it is all around stifled by the MTM structure as shown in Fig. 9. For this situation, maximum portion of the feed current is used to empower the emanating patch. This additional edge-to-edge coupling among patch and ground added radiation which helps to improve the bandwidth. By improving the shared coupling between components, the MTM structure hinders the surface waves.

A comparative study is done in TABLE II, in which BW improvement techniques are listed along with the substrate type, operating BW, gain, and size of the antenna. Compared to the literature of TABLE II, the proposed antenna is able to cover a large operating band with acceptable gain. The proposed antenna is compact and can operate in lower frequency region (1.5~10 GHz) compared to literature [7], [9], and [11-13]. Moreover, structures of literature [7] and [9] are more complex than the proposed design.

V. CONCLUSION

This paper proposed a bandwidth-enhanced antenna incorporating artificially designed unit cells of MTMs. A 1×2 array of the unit cell is integrated with the circular-shaped UWB monopole antenna. The monopole radiator can cover an ultra wide-band of 2.5 GHz to 10 GHz (impedance BW = 7.5 GHz) equivalent to a percentage bandwidth of 120%. Loading of MTMs results in band widened towards lower frequency region (1.5~3 GHz). The new impedance

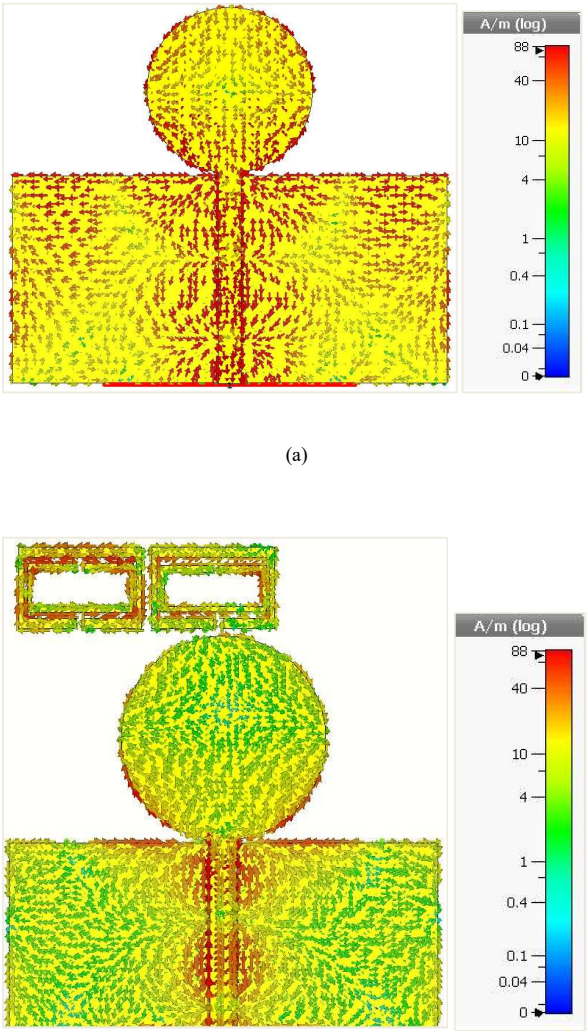

Fig. 9. Surface current distribution of the proposed antenna at 1.5 GHz. (a) without metamaterial array of unit cell, (b) with metamaterial array of unit cell.

bandwidth of the antenna is 1.5 GHz to 10 GHz (impedance BW = 8.5 GHz) equivalent to a percentage bandwidth of 147.8%. So, the percentage increase in bandwidth is 27.8%. The antenna gain in the 1.5~10 GHz frequency band is about 1.17~4.05 dBi. This design is compact, as it is possible to cover multiple wireless applications. The acquired performances of the suggested MTM UWB antenna bolstered and approved it as a foreseeable possibility for GPS 1.5 GHz, Wi-Fi 2.4 GHz, WiMax 2.5/3.5/5.5 GHz, WLAN 5.2/5.8 GHz, and X-band RADAR applications.

REFERENCES

[1] J. Liang, C. C. Chiau, X. Chen, and C. G. Parini, "Study of a printed circular disc monopole antenna for UWB systems," *IEEE trans. antennas propag.*, vol. 53, pp. 3500-3504, 2005.

[2] R. Garg, P. Bhartia, I. J. Bahl, and A. Ittipiboon, *Microstrip antenna design handbook*, Artech house, 2001.

[3] B.-L. Ooi, "A double-/spl Pi/stub proximity feed U-slot patch antenna," *IEEE trans. Antennas propag.*, vol. 52, pp. 2491-2496, 2004.

[4] A. Deshmukh and G. Kumar, "Broadband compact V-slot loaded RMSAs," *Electron. Lett.*, vol. 42, p. 1, 2006.

[5] V. G. Veselago, "Reviews of Topical Problems: the Electrodynamics of Substances with Simultaneously Negative Values of\epsilon and mu," *Sov. Phys. Uspekhi.*, vol. 10, p. R04, 1968.

[6] A. Grbic and G. V. Eleftheriades, "Experimental verification of backward-wave radiation from a negative refractive index metamaterial," *J. Appl. Phys*., vol. 92, pp. 5930-5935, 2002.

[7] T. Cai, G.-M. Wang, X.-F. Zhang, Y.-W. Wang, B.-F. Zong, and H.-X. Xu, "Compact microstrip antenna with enhanced bandwidth by loading magneto-electro-dielectric planar waveguided metamaterials," *IEEE Trans. Antennas Propag.*, vol. 63, pp. 2306-2311, 2015.

[8] B.-J. Niu, Q.-Y. Feng, and P.-L. Shu, "Epsilon negative zeroth-and first-order resonant antennas with extended bandwidth and high efficiency," *IEEE Trans. Antennas Propag.*, vol. 61, pp. 5878-5884, 2013.

[9] J. Zhu and G. V. Eleftheriades, "A compact transmission-line metamaterial antenna with extended bandwidth," *IEEE Antennas Wireless Propag. Lett.,* vol. 8, pp. 295-298, 2009.

[10] J. K. Ji, G. H. Kim, and W. M. Seong, "Bandwidth enhancement of metamaterial antennas based on composite right/left-handed transmission line," *IEEE Antennas Wireless Propag. Lett.,* vol. 9, pp. 36-39, 2010.

[11] K. K. Naik and P. A. V. Sri, "Design of hexadecagon circular patch antenna with DGS at Ku band for satellite communications," *Prog. Electromagn. Res*., vol. 63, pp. 163-173, 2018.

[12] L. H. Weng, Y.-C. Guo, X.-W. Shi, and X.-Q. Chen, "An overview on defected ground structure," *Prog. Electromagn. Res*., vol. 7, pp. 173-189, 2008.

[13] S. Elajoumi, A. Tajmouati, J. Zbitou, A. Errkik, A. Sanchez, and M. Latrach, "Bandwidth enhancement of compact microstrip rectangular antennas for UWB applications," *TELKOMNIKA.*, vol. 17, pp. 1559-1568, 2019.

[14] S. X. Ta, T. H. Y. Nguyen, K. K. Nguyen, and C. Dao-Ngoc, "Bandwidth-enhancement of circularly-polarized fabry-perot antenna using single-layer partially reflective surface," *Int. J. RF Microw. Comput.-Aided Eng.,* vol. 29, pp. 21774, 2019.

[15] M. Tamrakar and K. Usha Kiran, "Bandwidth enhancing method using tri-ring resonator metamaterial for small devices," *Microw. Opt. Technol. Lett.,* vol. 61, pp. 886-890, 2019.

[16] C. Arora, S. S. Pattnaik, and R. Baral, "Bandwidth Enhancement of Microstrip Patch Antenna Array Using Spiral Split Ring Resonator," in *Inf. Syst. Des. Intell. Applicat.*, Ed: Springer, pp. 435-441, 2018.

[17] W. Wu, B. Yuan, B. Guan, and T. Xiang, "A bandwidth enhancement for metamaterial microstrip antenna," *Microw. Opt. Technol. Lett.,* vol. 59, pp. 3076-3082, 2017.

[18] S. Kumari, S. Sachan, and A. Rajawat, "Bandwidth Enhancement of Microstrip Patch Antenna Using Disconnected U-Shaped DGS," in *Intell. Commun, Control Dev.*, Ed. Springer, pp. 1009-1018, 2018.

[19] S. Naoui, L. Latrach, and A. Gharsallah, "Equivalent circuit model of double Split ring resonators," *Microw. Opt. Technol. Lett.,* vol. 11, pp. 1-6, 2016.